N-tag probability law of the symmetric exclusion process

Alexis Poncet,[1] Olivier Bénichou,[1] Vincent Démery,[2,3] and Gleb Oshanin[1]
[1]*LPTMC, CNRS/Sorbonne Université, 4 Place Jussieu, F-75005 Paris, France*
[2]*Gulliver, CNRS, ESPCI Paris, PSL Research University, 10 rue Vauquelin, Paris, France*
[3]*Univ Lyon, ENS de Lyon, Univ Claude Bernard Lyon 1, CNRS, Laboratoire de Physique, F-69342 Lyon, France*

(Received 25 January 2018; revised manuscript received 18 April 2018; published 8 June 2018)

The symmetric exclusion process (SEP), in which particles hop symmetrically on a discrete line with hard-core constraints, is a paradigmatic model of subdiffusion in confined systems. This anomalous behavior is a direct consequence of strong spatial correlations induced by the requirement that the particles cannot overtake each other. Even if this fact has been recognized qualitatively for a long time, up to now there has been no full quantitative determination of these correlations. Here we study the joint probability distribution of an arbitrary number of tagged particles in the SEP. We determine analytically its large-time limit for an arbitrary density of particles, and its full dynamics in the high-density limit. In this limit, we obtain the time-dependent large deviation function of the problem and unveil a universal scaling form shared by the cumulants.

DOI: 10.1103/PhysRevE.97.062119

I. INTRODUCTION

Single-file diffusion refers to the motion of particles in narrow channels, in which the geometrical constraints do not permit the particles to bypass each other. The very fact that the initial order is maintained at all times leads to a subdiffusive behavior $\langle X_t^2\rangle \propto \sqrt{t}$ of the position of any tagged particle (TP) [1], as opposed to the regular diffusion scaling $\langle X_t^2\rangle \propto t$. This theoretical prediction has been experimentally observed by microrheology in zeolites, transport of confined colloidal particles, and dipolar spheres in circular channels [2–6].

A minimal model of single-file diffusion is the symmetric exclusion process (SEP). Here particles, present at a density ρ, perform symmetric continuous-time random walks on a one-dimensional lattice with unit jump rate, and hard-core exclusion is enforced by allowing at most one particle per site. A key result is that the long-time behavior of the variance of the position of a TP initially located at the origin obeys $\langle X_t^2\rangle \underset{t\to\infty}{\sim} \frac{1-\rho}{\rho}\sqrt{\frac{2t}{\pi}}$. The SEP has now become a paradigmatic model of subdiffusion in confined systems, and it has generated a huge number of works in the mathematical and physical literature (see, e.g., Refs. [7–13]). Recent advances include the calculation of the cumulants of X_t in the dense limit $\rho \to 1$ [14] or at long time for any density [15]. While the SEP in its original formulation provides a model of subdiffusion in crowded equilibrium systems, important extensions to nonequilibrium situations have recently been considered. In Ref. [15] all the cumulants of a symmetric TP immersed in a step initial profile with different densities of particles on the left and on the right of the TP are calculated. In the other intrinsically out-of-equilibrium situation of a driven TP in a SEP, the mean position [16,17] and all higher order moments in the dense limit [14] have been calculated and shown to grow anomalously like $\sqrt{t}$.

This collection of anomalous behaviors in the SEP is a direct consequence of strong spatial correlations in the single-file geometry. Even if this fact has been recognized qualitatively for a long time, up to now there is no full quantitative determination of these correlations. As a matter of fact, all the results mentioned above concern observables associated with a *single* TP. A complete characterisation of the correlations requires the knowledge of *several* TP observables. To date, the only available results concern the case of two TPs. Two-point correlation functions have been analyzed either by using a stochastic harmonic theory (Edwards-Wilkinson dynamics) [18] or for the so-called random average process [19,20], which displays several qualitative features similar to the dilute limit of the SEP. In the continuous space description, which can be seen as the dilute limit $\rho \to 0$ of the SEP, a two-tag probability distribution has been determined [21]. Here we study the full joint distribution of an arbitrary number N of TPs in the SEP and determine (1) the large-time limit for an arbitrary density of particles and (2) the full dynamics in the dense limit $\rho \to 1$.

We will call $X_i(t)$ the positions of the N TPs, $Y_i(t) = X_i(t) - X_i(0)$ their displacements, $L_i = X_{i+1}(0) - X_i(0)$ the initial distances, and $L = \sum_{i=1}^{N-1} L_i$ the total distance (Fig. 1).

II. ARBITRARY DENSITY

A. Identification of the time regimes

We first present a qualitative analysis of the dynamics of the correlations. In the short-time regime $t \ll L_j^2$ for all j (diffusive timescales are expected), the TPs are independent, so that the joint distribution can be factorized, in terms of the single-particle probability law P_1: $\mathbb{P}(\{Y_i\}) = \prod_{i=1}^N P_1(Y_i)$. In the large-time limit $t \gg L^2$, we will show with simple arguments that the distances between consecutive TPs are asymptotically stationary and the set of N TPs behaves as a single one, described by

$$\mathbb{P}(\{Y_i = y_i\sqrt{t}\}) \asymp e^{-\sqrt{t}I\left(\frac{y_1+\cdots+y_N}{N}\right)} \prod_{i=2}^{N} \delta(y_i - y_1), \qquad (1)$$

where $I(y)$ is the large deviation function of a single TP, defined by $P_1(Y = y\sqrt{t}) \asymp e^{-\sqrt{t}I(y)}$ and calculated very recently in Ref. [15] (the symbol "$\asymp$" stands for equivalence at

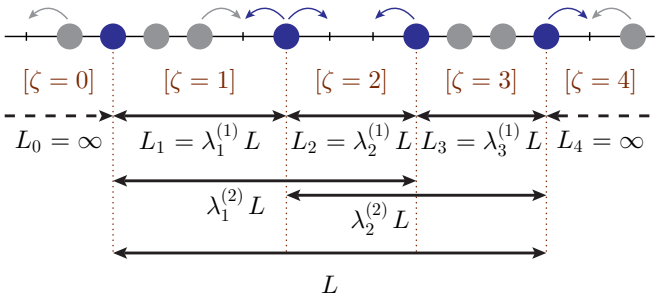

FIG. 1. Summary of our notations in the case of $N = 4$ TPs. The blue particles are the TPs, the gray ones are the other particles. The curved arrows show the allowed moves.

exponential order). A natural question then arises: what is the full behavior of the joint probability as a function of time between these two extremes? A large deviation function K depending on the rescaled time $\tau = t/L^2$ and the relative distances $\lambda_j^{(1)} = L_j/L$ is expected:

$$\mathbb{P}(\{Y_i = y_i\sqrt{t}\}) \asymp e^{-\sqrt{t}K\left(\{y_i\},\tau,\left\{\lambda_j^{(1)}\right\}\right)}. \tag{2}$$

In this paper we determine this large deviation function in the high-density limit and unveil a striking universal scaling form of the N-tag cumulants.

B. Behavior at large time

We start by showing that the large-time behavior of the distribution can be determined from general arguments, valid at any density ρ. A useful auxiliary step, interesting by itself, consists in determining the distribution of the distance between two neighboring TPs. The distance between two TPs, initially separated by L^*, can be written as $\Delta = k + m + 1$, where k is the number of particles between the TPs (fixed initially for a given realization), of law $P_{\rm part}(k)$, and m is the number of vacancies between the TPs, of law $P_{\rm vac}(m|k)$; hence the law P_Δ of Δ reads

$$P_\Delta(\Delta) = \sum_{k=0}^{L^*-1} P_{\rm part}(k) P_{\rm vac}(\Delta - k - 1|k). \tag{3}$$

We now note that, since there is a constant probability ρ of finding initially a particle on each of the $L-1$ sites between the TPs, k is a binomial random variable of law $P_{\rm part}(k) = \binom{L^*-1}{k}\rho^k(1-\rho)^{L^*-1-k}$. Then we remark that the number of vacancies between the TPs, knowing that there are k particles between the TPs, is equal to the number of times we "fail" to discover a particle before "finding" $k+1$ of them, which is the definition of a negative binomial random variable, of law $P_{\rm vac}(m|k) = \binom{m+k}{m}(1-\rho)^m\rho^{k+1}$. The law P_Δ from Eq. (3) is thus fully characterized and is checked to agree with numerical simulations (see Appendix A 1). Note that, as a consequence of Eq (3), the variation of the distance between TPs $D = \Delta - L^*$ can be shown to follow itself a large deviation principle $P_{\rm dist}(D = L^* d) \asymp e^{-L^* J(d)}$ with

$$J(d) = \sup_{v\in\mathbb{R}} \left\{ v(1+d) - \ln\left[\frac{\rho^2}{e^{-v} - (1-\rho)} + 1 - \rho\right]\right\}. \tag{4}$$

The distribution defined by Eq. (3) is stationary, which means that the moments of the variation of distance $\langle [Y_2(t) - Y_1(t)]^n\rangle$ have a well-defined limit at large time. We now note that the cumulants $\kappa^{(N)}_{p_1,\dots,p_N}(t)$ involving N TPs [see Eq. (10) for a precise definition] can be written as a sum of moments involving a single TP and moments involving distances. For instance, $\kappa^{(2)}_{11}(t) = \langle Y_1(t)Y_2(t)\rangle = \langle Y_1(t)^2\rangle + \langle Y_1(t)[Y_2(t) - Y_1(t)]\rangle$. We recall that $\langle Y_1(t)^2\rangle \propto \sqrt{t}$, while $\langle (Y_2(t) - Y_1(t))^2\rangle \propto t^0$. Applying finally the Cauchy-Schwarz inequality, we obtain that $\langle Y_1(t)[Y_2(t) - Y_1(t)]\rangle = O(t^{1/4})$. The large-time behavior of $\kappa^{(2)}_{11}(t)$ is thus given by the large-time behavior of the single TP cumulant of the same order, $\kappa^{(1)}_2(t) = \langle Y_1(t)^2\rangle$. This is true for all the cumulants (see Appendix A 3), leading finally to

$$\lim_{t\to\infty} \frac{\kappa^{(N)}_{p_1,\dots,p_N}}{\sqrt{t}} = \lim_{t\to\infty} \frac{\kappa^{(1)}_{p_1+\cdots+p_N}}{\sqrt{t}} \equiv B_{p_1+\cdots+p_N}, \tag{5}$$

where the constants B_k, involved in the single tagged particle problem, have been determined in Ref. [15].

Equation (5) implies that the group of N TPs behaves at long time like a single TP and proves Eq. (1). As we proceed to show by relying on the limit of a dense system, this single TP behavior holds only at very large time. Below we determine the complete dynamics of the joint distribution of the N TPs in the dense limit, which constitutes the core of this paper. We show that this dynamics is subtle and cannot be inferred from a single TP analysis.

III. DENSE LIMIT

A. Vacancy-based approach

Following Refs. [14,22–26], we focus on the limit of a dense system ($\rho \to 1$) and follow the evolution of the vacancies, rather than the particles, in a discrete time t. We assume that the vacancies perform symmetrical nearest-neighbor random walks and that particles move by exchanging their positions with the ones of the vacancies. We give here the main steps of the analysis. Detailed calculations can be found in Appendix B. We first consider a finite system of $\mathcal{N}$ sites and M vacancies, with N TPs. The probability $P^{(t)}(\mathbf{Y}|\{Z_j\})$ that the displacements of the TPs at time t are $\mathbf{Y}(t) = (Y_1(t),\dots,Y_N(t))$ knowing that the vacancies were initially located at $(Z_1,\dots,Z_M)$ can be written as a sum over the contributions of all vacancies

$$P^{(t)}(\mathbf{Y}|\{Z_j\}) = \sum_{\mathbf{Y}^1,\dots,\mathbf{Y}^M} \delta_{\mathbf{Y},\mathbf{Y}^1+\cdots+\mathbf{Y}^M} P^{(t)}(\{\mathbf{Y}^j\}|\{Z_j\}), \tag{6}$$

where $P^{(t)}(\{\mathbf{Y}^j\}|\{Z_j\})$ is the conditional probability that within the time interval t the TPs performed displacements $\mathbf{Y}^1$ (resp. $\mathbf{Y}^2,\dots$) due to the interaction with vacancy 1 (resp. 2, ...). In the high-density limit the vacancies contribute independently to the total displacement of the TPs, leading to

$$P^{(t)}(\{\mathbf{Y}^j\}|\{Z_j\}) \underset{\rho\to 1}{\sim} \prod_{j=1}^{M} p^{(t)}_{Z_j}(\mathbf{Y}^j), \tag{7}$$

where $p^{(t)}_Z(\mathbf{Y})$ is the probability that the displacements of the TPs are $\mathbf{Y}$ at time t due to a *single* vacancy that was initially at site Z. This factorization amounts to neglecting events

corresponding to two vacancies interacting simultaneously with the TPs. This approach is the discrete counterpart of the continuous-time version of the SEP in the dense limit and gives exact results at order $O(1-\rho)$.

Taking the Fourier transform of (6) and (7) with respect to $\mathbf{Y}$, averaging over the initial positions of the vacancies $\{Z_j\}$, and finally taking the thermodynamic limit $\mathcal{N}, M \to \infty$ with $\rho_0 \equiv 1-\rho = M/\mathcal{N}$ remaining constant, the second characteristic function

$$\psi^{(t)}(\mathbf{k}) \equiv \ln\left[\left\langle \sum_{\mathbf{Y}\in\mathbb{Z}^N} P^{(t)}(\mathbf{Y}|\{Z_j\})e^{i\mathbf{k}\cdot\mathbf{Y}}\right\rangle_{\{Z_j\}}\right] \tag{8}$$

is found to be given by

$$\lim_{\rho_0\to 0}\frac{\psi^{(t)}(\mathbf{k})}{\rho_0} = \sum_{Z\notin\{X_i(t=0)\}} \tilde{q}_Z^{(t)}(\mathbf{k}), \tag{9}$$

where $\tilde{q}_Z^{(t)}(\mathbf{k}) \equiv \tilde{p}_Z^{(t)}(\mathbf{k}) - 1$, $p_Z^{(t)}(\mathbf{k})$ being the Fourier transform of $p_Z^{(t)}(\mathbf{Y})$. By definition, ψ gives the N-tag cumulant of the displacements with coefficients $p_1,\dots,p_N$,

$$\kappa^{(N)}_{p_1,\dots,p_N} = (-i)^{p_1+\cdots+p_N}\left.\frac{\partial^{p_1+\cdots+p_N}\psi}{\partial k_1^{p_1}\dots\partial k_N^{p_N}}\right|_{\mathbf{k}=\mathbf{0}}. \tag{10}$$

The next step of the calculation consists in determining the single-vacancy probability $\tilde{q}_Z^{(t)}(\mathbf{k})$ involved in Eq. (9), by considering a system containing a single vacancy. A technical difficulty is that the distance between two TPs (j and $j+1$) is not constant. In our one-dimensional situation, at a given time, it can assume two values depending on the initial position Z of the vacancy: $L_j^{(\zeta(Z))} = L_j + 1$ if $\zeta(Z) \neq j$, or $L_j^{(\zeta(Z))} = L_j$ if $\zeta(Z) = j$. $\zeta(Z)$ denotes the "interval" in which the vacancy started: $\zeta(Z) = j$ if the vacancy starts between TP j and TP $j+1$, and $\zeta(Z) = 0$ [resp. $\zeta(Z) = N$] if it starts on the left (resp. on the right) (see Fig. 1).

The key to obtaining $\tilde{q}_Z^{(t)}(\mathbf{k})$ is to introduce the first-passage probability $F_{\eta,Z}^{(t)}$ that the vacancy that started from site Z at time 0 arrives for the first time to the position of one of the TPs at time t, conditioned by the fact that it was on the "adjacent site" η at the discrete time $t-1$. The adjacent site $\eta = i$ (resp. $\eta = -i$) is defined as the site to the right (resp. left) of the ith TP. In analogy with q_Z and $F_{\eta,Z}$, we introduce quantities related to an adjacent site ν: $q_\nu^{(t,\zeta)}$ and $F_{\eta,\nu}^{(t,\zeta)}$ (that depend on the distances between TPs, thus on ζ). One can now partition over the first passage of the vacancy to the site of one of the TPs to get an expression for $\tilde{q}_Z$:

$$\tilde{q}_Z^{(t)}(\mathbf{k}) = -\sum_{j=0}^{t}\sum_{\nu}\left\{1-\left[1+\tilde{q}_{-\nu}^{(t-j,\zeta(Z))}(\mathbf{k})\right]F_{\nu,Z}^{(j)}\right\}. \tag{11}$$

To obtain $\tilde{q}_\eta^{(t,\zeta)}$, we decompose the propagator of the displacements over the successive passages of the vacancy to the position of one of the TPs using $\mathbf{e}_{\pm 1} = (\pm 1,0,\dots),\dots,$ $\mathbf{e}_{\pm N} = (0,\dots,0,\pm 1)$ as a basis for the displacements $\mathbf{Y}$. This writes as a time convolution of quantities $F_{\eta,\nu}^{(t,\zeta)}$: the Laplace transform, $\hat{\tilde{q}}_\eta^{(\zeta)}(\mathbf{k},\xi) = \sum_{t=0}^{\infty}\xi^t\tilde{q}_\eta^{(t,\zeta)}(\mathbf{k})$, writes as an infinite sum of matrix powers, giving

$$\hat{\tilde{q}}_\eta^{(\zeta)}(\mathbf{k},\xi) = \frac{1}{1-\xi}\sum_{\mu,\nu}\{[1-T^{(\zeta)}(\mathbf{k},\xi)]^{-1}\}_{\nu\mu} \times(1-e^{-i\,\mathbf{k}\cdot\mathbf{e}_\nu})e^{i\,\mathbf{k}\cdot\mathbf{e}_\mu}\hat{F}_{\mu\eta}^{(\zeta)}(\xi). \tag{12}$$

The matrix T is defined by $T^{(\zeta)}(\mathbf{k},\xi)_{\nu\mu} = \hat{F}_{\nu,-\mu}^{(\zeta)}(\xi)e^{i\,\mathbf{k}\cdot\mathbf{e}_\nu}$.

Introducing Eq. (11) into Eq. (9), one gets an expression for the Laplace transform of the second characteristic function:

$$\lim_{\rho_0\to 0}\frac{\hat{\psi}(\mathbf{k},\xi)}{\rho_0} = -\sum_{\nu}\left\{\frac{1}{1-\xi}-\left[\frac{1}{1-\xi}+\hat{\tilde{q}}_{-\nu}^{(\zeta)}(\mathbf{k},\xi)\right]e^{i\,\mathbf{k}\mathbf{e}_\nu}\right\}h_\zeta(\xi) \tag{13}$$

$$h_\zeta(\xi) = \sum_{Z\notin\{X_i(t=0)\}}\hat{F}_{\zeta,Z}(\xi). \tag{14}$$

Here we defined $\zeta = \zeta(\nu)\in[0,N]$ by $\zeta = \nu$ if $\nu > 0$ and $\zeta = -\nu - 1$ if $\nu < 0$.

Finally, the quantities that we need are the probabilities to go from one adjacent site to another: $\hat{F}_{-1,-1} = \hat{F}_{+N,+N}$, $\hat{F}_{\mu,\mu}^{(\zeta)} = \hat{F}_{-(\mu+1),-(\mu+1)}^{(\zeta)}$, $\hat{F}_{\mu,-(\mu+1)}^{(\zeta)} = \hat{F}_{-(\mu+1),\mu}^{(\zeta)}$, and the sums $h_0 = h_N$ and h_μ ($\mu = 1,\dots,N-1$). The other $\hat{F}_{\nu,\eta}$ are zero. These quantities can be computed explicitly using classical results on first-passage times of symmetric one-dimensional random walks [27]. This completes the determination of the second characteristic function.

B. Characteristic function

Importantly, the characteristic function can be shown from Eq. (13) to admit the following simple form in the scaling limit $t\to\infty$, $L\to\infty$ with fixed rescaled time $\tau = t/L^2$ and fixed relative lengths $\lambda_i^{(1)} = L_i/L$:

$$\lim_{\rho_0\to 0}\frac{\psi(\mathbf{k},t)}{\rho_0} = \sqrt{\frac{2t}{\pi}}\sum_{n=0}^{N-1}\sum_{i=1}^{N-n}[\cos(k_i+\cdots+k_{i+n})-1] \times\left[g\left(\frac{\lambda_i^{(n)}}{\sqrt{2\tau}}\right)-g\left(\frac{\lambda_{i-1}^{(n+1)}}{\sqrt{2\tau}}\right) -g\left(\frac{\lambda_i^{(n+1)}}{\sqrt{2\tau}}\right)+g\left(\frac{\lambda_{i-1}^{(n+2)}}{\sqrt{2\tau}}\right)\right], \tag{15}$$

$$g(u) = e^{-u^2} - \sqrt{\pi}\,u\,\operatorname{erfc}(u), \tag{16}$$

where we have defined $\lambda_i^{(n)} = (L_i+\cdots+L_{i+n-1})/L$, $\lambda_i^{(0)} = 0$ and used the convention $L_0 = L_N = +\infty$ (Fig. 1).

Equation (15) gives us the full dynamics of the N-tag probability law of the SEP in the dense limit and is the main result of this paper. Note that it involves the $N(N-1)/2$ timescales $(\lambda_i^{(n)}L)^2$, associated to the initial distances between the N TPs. In the following we analyze two important consequences. First, we determine the large deviation function of the problem, which allows us to obtain quantitatively the joint distribution at any time. Second, we unveil a surprising universality property of the N-tag cumulants.

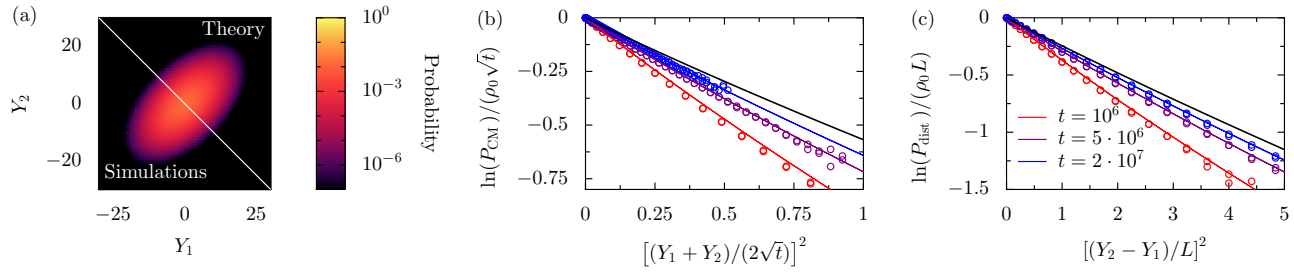

FIG. 2. Theory vs numerical simulations (relying on the dynamics of the vacancies) for $\rho = 0.01$ and $L = 10^3$. (a) Joint probability distribution of the displacements (Y_1, Y_2) of two TPs at $t = 5\times10^6$: numerical simulations vs theoretical prediction (17). (b) Rescaled marginal probability density of the center of mass displacement at times $t = 1\times10^6$, 5×10^6, 2×10^7 ($\tau = 1,5,20$). Numerical simulations (dots) vs theoretical prediction (lines). The black line is the prediction when $\tau \to \infty$ [Eq. (18)]. (c) Rescaled marginal probability density of the distance between TPs at the same times as (b). The black line is the prediction when $\tau \to \infty$ [Eq. (19)].

C. Time-dependent large deviation function

Noticing that $\psi(-i\mathbf{s},t) = \ln\langle e^{\mathbf{s}\cdot\mathbf{Y}(t)}\rangle$, it is possible to apply the Gärtner-Ellis theorem [28] to write the joint probability in the large-time limit under a large-deviation form

$$\mathbb{P}(\{Y_i = \rho_0\sqrt{t}\,y_i\},\tau) \asymp e^{-\rho_0\sqrt{t}\tilde{K}(\{y_i\},\tau)}, \tag{17}$$

$\tilde{K}(\{y_i\},\tau) = \sup_{\mathbf{s}\in\mathbb{R}^N}[\sum_{i=1}^N s_i y_i - (\rho_0\sqrt{t})^{-1}\psi(-i\mathbf{s})]$, $\psi(\mathbf{k})$ being given by (15). In other words, we have determined the dense limit of the large deviation function K introduced in (2), related to $\tilde{K}$ by $\tilde{K}(\{y_i\}) = \lim_{\rho_0\to0}\rho_0^{-1}K(\{\rho_0 y_i\})$. We stress that Eq. (17) gives the probability distribution of the TPs at *arbitrary* rescaled times. We checked it against numerical simulations and found a very good agreement [Fig. 2(a)].

To illustrate this result, we now focus on the marginal laws $P_{\rm CM}(Y_{\rm CM})$ and $P_{\rm dist}(D)$ of, respectively, the center of mass $Y_{\rm CM} = (Y_1 + \cdots + Y_N)/N$ and the variation of distance $D = Y_N - Y_1$. The full dynamics of these marginal laws can be extracted from Eq. (17) and is displayed in Figs. 2(b) and 2(c).

In these figures, the black curves represent the large-time limit ($\tau \to \infty$) of these two laws:

$$\lim_{\tau\to\infty} P_{\rm CM}\left(Y_{\rm CM} = \rho_0\sqrt{\frac{2t}{\pi}}\,y\right) \asymp e^{-\rho_0\sqrt{\frac{2t}{\pi}}I_0(y)} \tag{18}$$

$$\lim_{\tau\to\infty} P_{\rm dist}(D = 2\rho_0 L d) \asymp e^{-2\rho_0 L I_0(d)}, \tag{19}$$

where $I_0(u) = 1 - \sqrt{1+u^2} + u\ln(u+\sqrt{1+u^2})$. Parenthetically, this also corresponds to the high-density limit of Eqs. (1) and (4), which were obtained in the large-time regime $t \gg L^2$, noting that $\lim_{\rho_0\to0} I(\rho_0\sqrt{2/\pi}\,u)/(\rho_0\sqrt{2/\pi}) = I_0(u)$ and $\lim_{\rho_0\to0} J(2\rho_0 u)/(2\rho_0) = I_0(u)$. Figures 2(b) and 2(c) demonstrate that at finite time, there is a significant deviation with these asymptotic laws, quantified by our approach.

D. Universal scaling of the cumulants

A second striking consequence of Eq. (15) is that all the even N-tag cumulants ($p_1 + \cdots + p_N$ even in Eq. (10), with $p_1 \neq 0$ and $p_N \neq 0$) are equal and assume the following universal scaling form (the odd cumulants are equal to zero):

$$\lim_{\rho_0\to0}\frac{\kappa^{(N)}_{\rm even}(t)}{\rho_0} = \sqrt{\frac{2t}{\pi}}\,g\left(\frac{1}{\sqrt{2\tau}}\right) + o(\sqrt{t}); \tag{20}$$

g was defined in Eq. (16). This expression gives back the expected large-time behavior Eq. (5) and is found to be in very good agreement with continuous-time simulations of the SEP at any rescaled time (Fig. 3). Several comments are in order. (1) A major result is that the scaling form Eq. (20) is universal with respect to the indices of the cumulant, the number of TPs, and the initial configurations of TPs for a fixed separation L of extreme TPs. In particular, the cumulants do not depend on the collection of timescales $(\lambda_i^{(n)}L)^2$ introduced above but only on L^2. (2) This result is highly nontrivial as best appreciated by comparing to the cumulants of the center-of-mass position, which can be obtained from Eq. (15); the dynamics of these cumulants does not share any of these universality properties, and in particular does not admit a simple scaling form with a single timescale (see Appendix A 4 and Fig. 3 inset, $\kappa^{(N)}_{{\rm CM},p}$ denotes the pth cumulant of the center of mass of N particles). (3) This universal behavior is a high-density effect, the dynamics of the cumulants for an arbitrary density of particles being nonuniversal (see Appendix C 4). (4) The Edwards-Wilkinson equation, which is seen as the

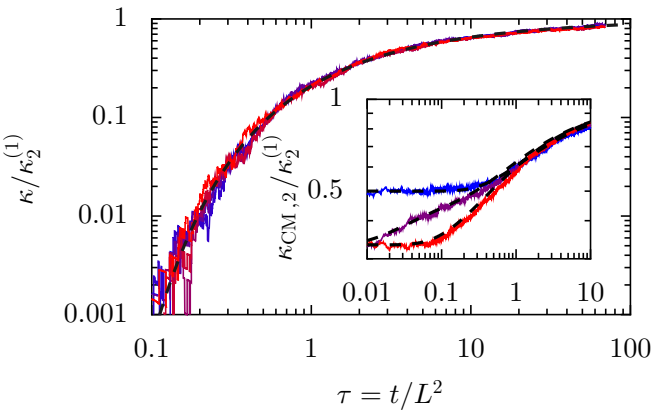

FIG. 3. Rescaled evolution of the cumulants associated to two to four TPs at $\rho_0 = 0.002$ and $L = 12$ (24 for the inset). Main figure: simulations in continuous time, from blue to red: $\kappa^{(2)}_{11}$, $\kappa^{(2)}_{22}$, $\kappa^{(2)}_{31}$, $\kappa^{(3)}_{121}$, $\kappa^{(3)}_{211}$, $\kappa^{(4)}_{1111}$; black curve: prediction from Eq. (20). Inset: rescaled variance of the center of mass, from blue to red: $\kappa^{(2)}_{\rm CM,2}$, $\kappa^{(3)}_{\rm CM,2}$ ($\lambda_1^{(1)} = 1/6$, $\lambda_2^{(1)} = 5/6$), $\kappa^{(3)}_{\rm CM,2}$ ($\lambda_1^{(1)} = \lambda_2^{(1)} = 0.5$); the black lines are the predictions. We recall that $\kappa_2^{(1)} = \rho_0\sqrt{2t/\pi}$.

Gaussian limit of the SEP [29,30], provides the first two cumulants and leads to $\kappa_{11}^{(2)} = \kappa_2^{(1)} g[(2\tau)^{-1/2}]$ at any density [18,31], consistently with Eq. (20). A similar scaling for $\kappa_{11}^{(2)}$ has also been found in the random average process [19,20]. Here this scaling form is shown to hold for *all* the cumulants and for an *arbitrary* number of TPs.

IV. CONCLUSION

To sum up, we studied the joint probability distribution of an arbitrary number of tagged particles in the SEP. In the large-time regime, this distribution can be obtained by simple arguments at any density of particles and displays a single tracer behavior. The regime of intermediate times is more subtle. In the dense limit of particles, we obtained the full dynamics and explicitly derived the time-dependent large deviation function of the problem. We also unveiled a universal scaling form shared by all cumulants.

APPENDIX A: DYNAMICS AT ARBITRARY DENSITY

1. Law of the distance between two particles

In this appendix, we explain in detail the steps leading to the distribution of the distance between two TPs [Eq. (3)].

We consider two tagged particles (TPs) in the SEP with density ρ. The initial distance between them is L^*, and we derive the equilibrium distribution P_Δ of the distance Δ (in particular we show that the distribution of the distance is time-independent at large time). We proceed as follows: (1) We write the law $P_{\rm part}$ of the number of particles k between the TPs. This number is fixed initially and does not evolve. (2) We write the law $P_{\rm vac}$ of the number of vacancies m between the tracers at equilibrium; this law depends on k.

As $\Delta = k + m + 1$ (see Fig. 4), we have

$$P_\Delta(\Delta) = \sum_{k=0}^{L^*-1} P_{\rm part}(k) P_{\rm vac}(\Delta - k - 1|k). \tag{A1}$$

Initially there are $L^* - 1$ sites between the TPs. Each site is occupied with probability ρ. This gives us a binomial law for N_p:

$$P_{\rm part}(k) = \binom{L^*-1}{k} \rho^k (1-\rho)^{L^*-1-k}. \tag{A2}$$

Now, we want to determine, at large time, the number of vacancies m between the two TPs ("left TP" and "right TP"), knowing that there are k particles between them. We explore the sites starting from the site on the right of the "left TP," and we travel to the right. At each site, we play a game and discover a particle with probability ρ. The $(k+1)$-th particle that is found is, by definition, the "right TP." The number of vacancies m is the number of times we failed to discover a particle. The process of counting the number m of failures before obtaining $k+1$ successes, when the probability of a success is ρ, corresponds by definition to a negative binomial law:

$$P_{\rm vac}(m|k) = \binom{m+k}{m} (1-\rho)^m \rho^{k+1}. \tag{A3}$$

Equivalently, one can see this negative binomial law as the law of the sum of $k+1$ independent geometric random variables.

From Eq. (A2), we obtain

$$P_\Delta(\Delta) = \sum_{k=0}^{L^*-1} P_{\rm part}(k) P_{\rm vac}(\Delta - k - 1|k) \tag{A4}$$

$$= \sum_{k=0}^{L^*-1} \binom{L^*-1}{k} \rho^k (1-\rho)^{L^*-1-k} \binom{\delta-1}{\Delta-k-1} (1-\rho)^{\Delta-k-1} \rho^{k+1} \tag{A5}$$

$$= \sum_{k=0}^{L^*-1} \binom{L^*-1}{k} \binom{\Delta-1}{k} \rho^{2k+1} (1-\rho)^{L^*+\Delta-2k-2}. \tag{A6}$$

This law is in very good agreement with the numerical simulations (Fig. 5).

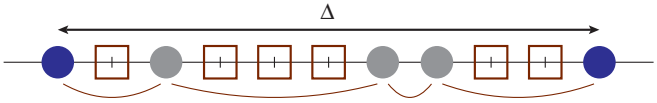

FIG. 4. Computation of the probability law of the distance between two TPs (blue circles). The distance is the sum of the number of particles in between (gray circles) and the number of vacancies (brown squares). The number k of particles (here $k = 3$) is fixed for any given system according to a binomial distribution. The total number of vacancies is the sum of the number of vacancies in each interval (brown curves). At equilibrium, it is given by a negative binomial distribution (see text).

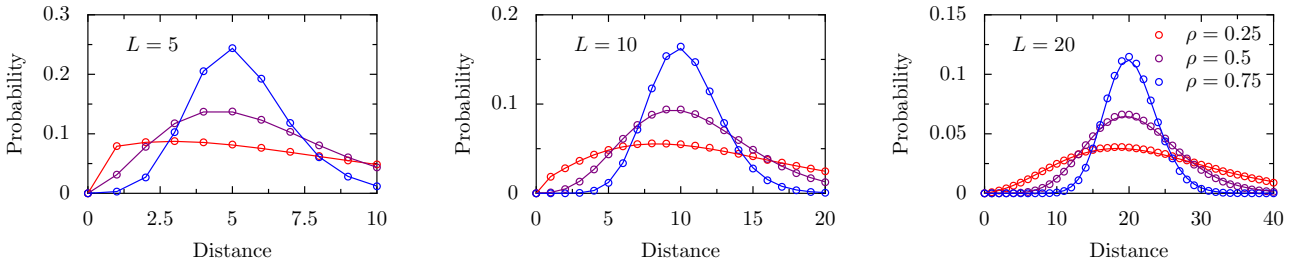

FIG. 5. Comparison of the numerical probability distribution of the distance of two TPs (dots) with the prediction (A6) (lines) for $\rho = 0.25,\ 0.5,\ 0.75$, and $L = 5,10,20$. The average is performed other 10^6 simulations at final time $t = 2\times10^4$ (we checked that this is enough for the convergence).

2. Large deviations of the law of the distance between two particles

We now prove Eq. (4) that gives the large deviation function of the distance computed above. We then show that this large deviation function is in agreement with our results at high density [Eq. (18)].

From the law of the distance (A6), one can derive the generating function $G_D(z)$:

$$G_D(z) \equiv \sum_{\Delta=1}^{\infty} P_\Delta(\Delta) z^\Delta \tag{A7}$$

$$= \sum_{\Delta=1}^{\infty} z^\Delta \sum_{k=0}^{L^*-1} P_{\text{part}}(k) P_{\text{vac}}(\Delta - k - 1|k) \tag{A8}$$

$$= z \sum_{k=0}^{L^*-1} z^k P_{\text{part}}(k) \sum_{m=0}^{\infty} z^m P_{\text{vac}}(m|k) \tag{A9}$$

$$= z \sum_{k=0}^{L^*-1} z^k \binom{L^*-1}{k} \rho^k (1-\rho)^{L^*-1-k} \sum_{m=0}^{\infty} \binom{m+k}{m} (1-\rho)^m \rho^{k+1} \tag{A10}$$

$$= z \sum_{k=0}^{L^*-1} z^k \binom{L^*-1}{k} \rho^k (1-\rho)^{L^*-1-k} \left[\frac{\rho}{1-(1-\rho)z}\right]^{k+1} \tag{A11}$$

$$= \left[\frac{\rho z}{1-(1-\rho)z}\right] \left[\frac{\rho^2 z}{1-(1-\rho)z} + 1 - \rho\right]^{L^*-1}. \tag{A12}$$

In the limit $L^* \to \infty$,

$$\frac{1}{L^*} \ln G_D(e^v) \xrightarrow[L^*\to\infty]{} \ln \left[\frac{\rho^2 e^v}{1-(1-\rho)e^v} + 1 - \rho\right] \equiv \phi(v). \tag{A13}$$

This enables us to apply the Gärtner-Ellis theorem of large deviations [28]. We write the result for the variation of distance $D = \Delta - L^*$: $P_{\text{dist}}(D) = P_\Delta(L^* + \Delta)$:

$$P_{\text{dist}}(D = L^* d) \asymp e^{-L^* J(d)}, \tag{A14}$$

$$J(d) = \sup_{v\in\mathbb{R}} [v(1+d) - \phi(v)] = \sup_{v\in\mathbb{R}} \left\{ v(1+d) - \ln\left[\frac{\rho^2}{e^{-v} - (1-\rho)} + 1 - \rho\right]\right\}. \tag{A15}$$

This the large deviation function given in Eq. (4).

High-density limit

Now we consider the high-density limit: $\rho = 1 - \rho_0$ with $\rho_0 \ll 1$. We obtain

$$\phi(v) = v + 2\rho_0 \cosh v + O\left(\rho_0^2\right). \tag{A16}$$

Thus, the supremum in (A15) is at v^* such that

$$\sinh v^* = \frac{d}{2\rho_0}. \tag{A17}$$

Introducing (A17) into (A15) we eventually obtain

$$J(d) = 2\rho_0 \left\{ 1 - \sqrt{1 + \left(\frac{d}{2\rho_0}\right)^2} + \frac{d}{2\rho_0} \log \left[\frac{d}{2\rho_0} + \sqrt{1 + \left(\frac{d}{2\rho_0}\right)^2} \right] \right\}. \tag{A18}$$

In other words,

$$\lim_{\rho_0 \to 0} \frac{J(2\rho_0 u)}{2\rho_0} = I_0(u) \tag{A19}$$

with $I_0(u) = 1 - \sqrt{1+u^2} + u \ln (u + \sqrt{1+u^2})$ as defined before. This is exactly what is found at large time with the high-density approach [Eq. (18)]. This result is used for the limiting (black) curve of Fig. 2(c).

3. Large-time behavior of the cumulants of N particles

The proof of the large-time scaling of the cumulants [Eq. (5)] has been given only for $\langle Y_1 Y_2 \rangle$. We now show that the result is valid for arbitrary cumulants.

We know that the moments of a single particle scale as $t^{1/2}$ [15]. On the other hand, the very fact that we found an asymptotic law for the distance (A6) implies that the moments of the distance scale as t^0 (the variance, the fourth moment, etc. have a well-defined limit). The large-time value of these moments can be computed from the generating function (A12).

Thus, our starting point is

$$\left\langle Y_1^{2p} \right\rangle = O(t^{1/2}), \quad \forall p \in \mathbb{N}. \tag{A20}$$

$$\langle (Y_i - Y_1)^{2p} \rangle = O(t^0), \quad \forall i \leqslant N, \forall p \in \mathbb{N}. \tag{A21}$$

From this we want to show that

$$A^{(N)}_{p_1,\dots p_N} \equiv \left\langle Y_1^{p_1} \cdots Y_N^{p_N} \right\rangle - \left\langle Y_1^{p_1+\cdots+p_N} \right\rangle = O(t^{1/4}), \quad \forall p_1, \dots, p_N. \tag{A22}$$

We proceed by induction: the case $N = 1$ is straightforward. Now assuming that (A22) holds for a given N, we want to prove it for $N+1$. As we have $A^{(N+1)}_{p_1,\dots p_N,0} = A^{(N)}_{p_1,\dots p_N} = O(t^{1/4})$, we prove by (another) induction (on q) that $A^{(N+1)}_{p_1,\dots p_N,q} = O(t^{1/4})\ \forall q \geqslant 0$. Indeed, if $A^{(N+1)}_{p_1,\dots p_N,q'} = O(t^{1/4})\ \forall q' < q$ (inductive hypothesis), we can write

$$A^{(N+1)}_{p_1,\dots p_N,q} = \left\langle Y_1^{p_1} \cdots Y_N^{p_N} Y_{N+1}^{q} \right\rangle - \left\langle Y_1^{p_1+\cdots+p_N+q} \right\rangle \tag{A23}$$

$$= \left\langle Y_1^{p_1} \cdots Y_N^{p_N} \left[(Y_{N+1} - Y_1)^q - \sum_{r=1}^{q} \binom{q}{r} (-1)^r Y_1^r Y_{N+1}^{q-r} \right] \right\rangle - \left\langle Y_1^{p_1+\cdots+p_N+q} \right\rangle \tag{A24}$$

$$= \left\langle Y_1^{p_1} \cdots Y_N^{p_N} (Y_{N+1} - Y_1)^q \right\rangle - \sum_{r=1}^{q} \binom{q}{r} (-1)^r \left\langle Y_1^{p_1+r} Y_2^{p_2} \cdots Y_{N+1}^{q-r} \right\rangle - \left\langle Y_1^{p_1+\cdots+p_N+q} \right\rangle \tag{A25}$$

$$= \left\langle Y_1^{p_1} \cdots Y_N^{p_N} (Y_{N+1} - Y_1)^q \right\rangle - \sum_{r=1}^{q} \binom{q}{r} (-1)^r \left[\left\langle Y_1^{p_1+r} Y_2^{p_2} \cdots Y_{N+1}^{q-r} \right\rangle - \left\langle Y_1^{p_1+\cdots+p_N+q} \right\rangle \right]. \tag{A26}$$

All the terms in the sum are of order $O(t^{1/4})$ from the inductive hypothesis (A22), and the first term can be bounded by the Cauchy-Schwarz inequality:

$$\left| \left\langle Y_1^{p_1} \cdots Y_N^{p_N} (Y_{N+1} - Y_1)^q \right\rangle \right| \leqslant \sqrt{\left\langle \left(Y_1^{p_1} \cdots Y_N^{p_N} \right)^2 \right\rangle \langle (Y_{N+1} - Y_1)^{2q} \rangle} = \sqrt{O(t^{1/2}) O(t^0)} = O(t^{1/4}) \tag{A27}$$

using (A20), (A21), and (A22). This ends the proof of (A22).

This implies that if $p_1 + \cdots + p_N$ is even:

$$\left\langle Y_1^{p_1} \cdots Y_N^{p_N} \right\rangle \underset{t \to \infty}{\sim} \left\langle Y_1^{p_1+\cdots+p_N} \right\rangle = O(t^{1/2}). \tag{A28}$$

The moments of N particles are equal, in the large-time limit, and are given by the moments of a single particle. This extends to the cumulants $\kappa^{(N)}_{p_1,\dots,p_N}$ defined from the second characteristic function:

$$\psi(k_1,\dots,k_N) \equiv \sum_{p_1,\dots p_N} \kappa^{(N)}_{p_1,\dots,p_N} \frac{(ik_1)^{p_1}\cdots(ik_N)^{p_N}}{p_1!\cdots p_N!} \equiv \log\left[\sum_{p_1,\dots p_N} \left\langle Y_1^{p_1}\cdots Y_N^{p_N}\right\rangle \frac{(ik_1)^{p_1}\cdots(ik_N)^{p_N}}{p_1!\cdots p_N!}\right], \tag{A29}$$

$$\kappa^{(N)}_{p_1,\dots,p_N} \underset{t\to\infty}{\sim} \kappa^{(1)}_{p_1+\cdots+p_N} \underset{t\to\infty}{\sim} B_{p_1+\cdots+p_N}\sqrt{t}, \tag{A30}$$

The coefficient B_p are computed in Ref. [15].

4. Motion of the center of mass in the limits of short and large time

As an illustration of the different time regimes, we now write the limits of the moments (or cumulants) of the center of mass at short and large time.

As the SEP is diffusive, the limit of large time, at which the cumulants reach their asymptotic scaling, is defined as $t \gg L^2$ where $L = X_N(t=0) - X_1(t=0)$ is the initial distance between the extreme TPs. The previous part implies that in this limit the cumulants $\kappa^{(N)}_{\mathrm{CM},p}$ (N is the number of TPs, p the order of the cumulant) of the displacement of the center of mass $(Y_1+\cdots+Y_N)/N$ of N TPs are equal to those of a single particle:

$$\left\langle\left(\frac{Y_1+\cdots+Y_N}{N}\right)^p\right\rangle = \frac{1}{N^p}\sum_{k_1+\cdots+k_N=p}\binom{p}{k_1,\dots,k_N}\left\langle Y_1^{k_1}\cdots Y_N^{k_N}\right\rangle \tag{A31}$$

$$\underset{t\to\infty}{\sim} \frac{1}{N^p}\sum_{k_1+\cdots+k_N=p}\binom{p}{k_1,\dots,k_N}\left\langle Y_1^{p}\right\rangle \tag{A32}$$

$$\underset{t\to\infty}{\sim} \left\langle Y_1^p\right\rangle \tag{A33}$$

$$\kappa^{(N)}_{\mathrm{CM},p} \underset{t\to\infty}{\sim} \kappa^{(1)}_{p} \underset{t\to\infty}{\sim} B_p\sqrt{t}. \tag{A34}$$

The multinomial coefficients are defined by $\binom{p}{k_1,\dots,k_N} = \frac{p!}{k_1!\dots k_N!}$. The sum runs over the N-tuples $(k_1,\dots,k_N)$ that verify $k_1+\cdots+k_N = p$. $\kappa^{(1)}_p$ is, again, the cumulant of order p of a single particle.

Using again the fact that the SEP is diffusive, we define the limit of small time as $t \ll L^2_{\min}$ (or equivalently $L_{\min} \gg \sqrt{t}$) where $L_{\min} = \min_{1\leqslant j\leqslant N-1} L_j$, $L_j = X_{j+1}(t=0) - X_j(t=0)$. In this limit, the TPs are independent from one another and the moments factorize:

$$\left\langle Y_1^{k_1}\cdots Y_N^{k_N}\right\rangle = \left\langle Y_1^{k_1}\right\rangle\cdots\left\langle Y_N^{k_N}\right\rangle. \tag{A35}$$

This implies the following formula for the cumulants of the center of mass:

$$\kappa^{(N)}_{\mathrm{CM},p} \underset{t\ll L^2_{\min}}{\sim} \frac{1}{N^{p-1}}\kappa^{(1)}_p. \tag{A36}$$

To summarize:

$$\kappa^{(N)}_{\mathrm{CM},p} = \begin{cases} \frac{1}{N^{p-1}}\kappa^{(1)}_p & \text{at short time} \\ \kappa^{(1)}_p & \text{at large time} \\ \kappa^{(N)}_{\mathrm{CM},p}\left(t, \frac{t}{L^2}, \left\{\frac{L_j}{L}\right\}\right) & \text{at intermediate time} \end{cases}. \tag{A37}$$

Our approach at high density enables us to obtain the intermediate time scaling. Note that the asymptotic scalings are recovered (numerically and theoretically) in the inset of Fig. 3.

APPENDIX B: DETAILED CALCULATIONS IN THE HIGH-DENSITY LIMIT

In this appendix we explain and prove the intermediate results of the high-density approach [Eqs. (6) to (14)]. We also derive explicit expressions for the quantities $\hat{F}^{(\zeta)}_{\mu,\nu}$ and h_μ that are involved.

1. Approximation and thermodynamic limit

Let us consider a system of size $\mathcal{N}$ with M vacancies and denote by $\mathbf{Y}(t) = [X_i(t) - X_i^0]_{i=1}^N$ the vector of the displacements of the TPs $[X_i^0 = X_i(t=0)]$. The probability $P^{(t)}(\mathbf{Y}|\{Z_j\})$ of having displacements $\mathbf{Y}$ at time t knowing that the M vacancies started at sites $Z_1\dots Z_M$ can be deduced from the displacements $\mathbf{Y}^i$ due to each vacancy i ($\mathbf{Y}^1$ is the vector of the displacements

induced by vacancy 1, $\mathbf{Y}^2$ the vector of the displacements induced by vacancy 2, etc.). We set $\mathbf{Y} = \mathbf{Y}^1 + \cdots + \mathbf{Y}^m$ and write

$$P^{(t)}(\mathbf{Y}|\{Z_j\}) = \sum_{\mathbf{Y}_1,\ldots,\mathbf{Y}_M} \delta_{\mathbf{Y},\mathbf{Y}_1+\cdots+\mathbf{Y}_M} \mathcal{P}^{(t)}(\{\mathbf{Y}^j\}|\{Z_j\}), \tag{B1}$$

where $\mathcal{P}^{(t)}(\{\mathbf{Y}^j\}|\{Z_j\})$ is the probability of displacement $\mathbf{Y}_j$ due to the vacancy j (for all j) knowing the initial positions $\{Z_j\}$ of all the vacancies.

Assuming that in the large density limit ($\rho \to 1$) the vacancies interact independently with the TPs, we can link it to the probability $p_Z^{(t)}(\mathbf{Y})$ that the tracers have moved by $\mathbf{Y}$ at time t due to a single vacancy that was initially at site Z; the probability law factorizes:

$$\mathcal{P}^{(t)}(\{\mathbf{Y}^j\}|\{Z_j\}) \underset{\rho\to 1}{\sim} \prod_{j=1}^{M} p_{Z_j}^{(t)}(\mathbf{Y}^j), \tag{B2}$$

so that Eq. (B1) becomes

$$P^{(t)}(\mathbf{Y}|\{Z_j\}) \underset{\rho\to 1}{\sim} \sum_{\mathbf{Y}^1,\ldots,\mathbf{Y}^M} \delta_{\mathbf{Y},\mathbf{Y}^1+\cdots+\mathbf{Y}^M} \prod_{j=1}^{M} p_{Z_j}^{(t)}(\mathbf{Y}^j). \tag{B3}$$

We take the Fourier transform, and we average over the initial positions of the vacancies:

$$\tilde{p}^{(t)}(\mathbf{k}) \equiv \frac{1}{\mathcal{N}-N} \sum_{Z\notin\{X_i^0\}} \sum_{\mathbf{Y}} p_Z^{(t)}(\mathbf{Y}) e^{i\mathbf{k}\mathbf{Y}} \tag{B4}$$

and *mutatis mutandis* for $\tilde{P}^{(t)}(\mathbf{k})$. Furthermore we write $\tilde{p}_Z^{(t)}(\mathbf{k}) = 1 + \tilde{q}_Z^{(t)}(\mathbf{k})$ (q_Z corresponds to the deviation from a Dirac function centered in 0):

$$\tilde{P}^{(t)}(\mathbf{k}) \underset{\rho\to 1}{\sim} [\tilde{p}^{(t)}(\mathbf{k})]^M = \left[\frac{1}{\mathcal{N}-N} \sum_{Z\notin\{X_i^0\}} \tilde{p}_Z^{(t)}(\mathbf{k})\right]^M = \left[1 + \frac{1}{\mathcal{N}-N} \sum_{Z\notin\{X_i^0\}} \tilde{q}_Z^{(t)}(\mathbf{k})\right]^M. \tag{B5}$$

We now take the limit $\mathcal{N}, M \to \infty$ with $\rho_0 \equiv 1-\rho = M/\mathcal{N}$ (density of vacancies) and N remaining constant. The second characteristic function reads

$$\lim_{\rho_0\to 0} \frac{\psi^{(t)}(\mathbf{k})}{\rho_0} \equiv \lim_{\rho_0\to 0} \frac{\ln[\tilde{P}^{(t)}(\mathbf{k})]}{\rho_0} = \sum_{Z\notin\{X_i^0\}} \tilde{q}_Z^{(t)}(\mathbf{k}). \tag{B6}$$

2. Expression of the single-vacancy propagator

We now consider the case of a single vacancy. To do the computation of $\tilde{q}_Z$, we introduce the following notations:

(1) As we will need to consider the passages of the vacancy to the site of one of the TPs, we consider the "adjacent sites" to the TPs, written with a Greek letter (η, ν, μ). $\eta = +i$ ($i = 1, \ldots, N$) denotes the site immediately to the right of TP i, while $\eta = -i$ denotes the site immediately to the left of TP i (see Fig. 6).

(2) $p_\eta^{(t)}(\mathbf{Y})$ is the probability that the tracers have moved by $\mathbf{Y}$ at time t knowing that the vacancy was initially on the adjacent site η.

(3) The probability that the vacancy is for the first time on the adjacent site η at time t knowing that it started from the site Z (resp. from the adjacent site ν) is denoted $F_{\eta,Z}^{(t)}$ (resp. $F_{\eta,\nu}^{(t)}$).

(4) As can be seen in Fig. 6, the distances between particles change (by a maximum of one unit) when the vacancy moves. More precisely, if we denote $\zeta \in [0, N]$ the interval in which the vacancy started (see main text and in particular Fig. 1 for further explanation), the "relevant" distance between particle j and particle $j+1$ is $L_j^{(\zeta)} = L_j + 1$ if $\zeta \neq j$, or

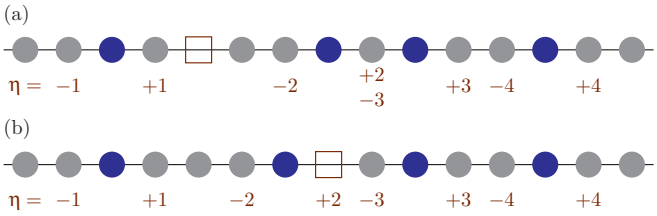

FIG. 6. Single vacancy case. The blue circles are the TPs, the brown square is the vacancy. Panels (a) and (b) show the same system at two different times. We define the "adjacent sites" $\eta = \pm 1, \ldots, \pm 4$ as the sites on the left and right of the TPs at a given time. Comparing (a) and (b) we see that the distances between TPs (e.g., the distance between TP 2 and TP 3) depend on the position of the vacancy; we account for this fact with the parameter ζ defined in the text.

$L_j^{(\zeta)} = L_j$ if $\zeta = j$. "Relevant" distance means the distance to be considered when the vacancy is, at some point, between the two particles (otherwise the distance is not involved in our calculation). In the following we write explicitly when a quantity depends on ζ.

Now, one can partition over the first passage of the vacancy to the site of one of the tracers to get an expression for $\tilde{q}_Z$ which is the main quantity involved in (B6):

$$p_Z^{(t)}(\mathbf{Y}) = \delta_{\mathbf{Y},\mathbf{0}}\left(1 - \sum_{j=0}^{t}\sum_{\nu=\pm1,\pm2} F_{\nu,Z}^{(j)}\right) + \sum_{j=0}^{t}\sum_{\nu=\pm1,\pm2} p_{-\nu}^{(t-j)}(\mathbf{Y})F_{\nu,Z}^{(j)}, \tag{B7}$$

$$\tilde{p}_Z^{(t)}(\mathbf{k}) = 1 - \sum_{j=0}^{t}\sum_{\nu=\pm1,\pm2} F_{\nu,Z}^{(j)} + \sum_{j=0}^{t}\sum_{\nu=\pm1,\pm2} \tilde{p}_{-\nu}^{(t-j,\zeta)}(\mathbf{k})F_{\nu,Z}^{(j)}, \tag{B8}$$

$$\tilde{q}_Z^{(t)}(\mathbf{k}) = -\sum_{j=0}^{t}\sum_{\nu=\pm1,\pm2} \left\{1 - \left[1 + \tilde{q}_{-\nu}^{(t-j,\zeta)}(\mathbf{k})\right]F_{\nu,Z}^{(j)}\right\}. \tag{B9}$$

An exponent ζ to a quantity means that this quantity is computed taking into account $\zeta = \zeta(Z)$.

We now need an expression for $\tilde{q}_\eta^\zeta$ where η is a special site. To do so we decompose the propagator of the displacements over the successive passages of the vacancy to the position of one of the tracers:

$$p_\eta^{(t),\zeta}(\mathbf{Y}) = \delta_{\mathbf{Y},\mathbf{0}}\left(1 - \sum_{j=0}^{t}\sum_{\mu} F_{\mu,\eta}^{(j,\zeta)}\right) + \sum_{p=1}^{\infty}\sum_{m_1,\ldots,m_p=1}^{\infty}\sum_{m_{p+1}=0}^{\infty}\delta_{t,\sum_i m_i}\sum_{\nu_1,\ldots,\nu_p}\delta_{\mathbf{Y},\sum_i \mathbf{e}_{\nu_i}}\left(1 - \sum_{j=0}^{m_{p+1}}\sum_{\mu} F_{\mu,-\nu_p}^{(j,\zeta)}\right)$$
$$\times F_{\nu_p,-\nu_{p-1}}^{(m_p,\zeta)}\cdots F_{\nu_2,-\nu_1}^{(m_2,\zeta)}F_{\nu_1,\eta}^{(m_1,\zeta)}; \tag{B10}$$

the sums on μ and ν_i run over the special sites $(\pm1,\ldots,\pm N)$.

The discrete Laplace transform (power series) of a function of time $g(t)$ is $\hat{g}(\xi) \equiv \sum_{t=0}^{\infty} g(t)\xi^t$. We can now take successively the Laplace and Fourier transforms of (B10) to get

$$\hat{p}_\eta^{(\zeta)}(\mathbf{Y},\xi) = \frac{1}{1-\xi}\left\{\delta_{\mathbf{Y},\mathbf{0}}\left(1 - \sum_{\mu}\hat{F}_{\mu,\nu}^{(\zeta)}\right) + \sum_{p=1}^{\infty}\sum_{\nu_1,\ldots,\nu_p}\delta_{\mathbf{Y},\sum_i \mathbf{e}_{\nu_i}}\sum_{\mu}\left(1 - \hat{F}_{\mu,-\nu_p}^{(\zeta)}\right)\hat{F}_{\nu_p,-\nu_{p-1}}^{(\zeta)}\cdots\hat{F}_{\nu_2,-\nu_1}^{(\zeta)}\hat{F}_{\nu_1,\eta}^{(\zeta)}\right\} \tag{B11}$$

$$\hat{\tilde{q}}_\eta^{(\zeta)}(\mathbf{k},\xi) \equiv \hat{\tilde{p}}_\eta^{(\zeta)}(\mathbf{k},\xi) - \frac{1}{1-\xi} = \frac{1}{1-\xi}\sum_{\mu,\nu}\{[1 - T^{(\zeta)}(\mathbf{k},\xi)]^{-1}\}_{\nu\mu} \times (1 - e^{-i\,\mathbf{k}\mathbf{e}_\nu})e^{i\,\mathbf{k}\mathbf{e}_\mu}\hat{F}_{\mu\eta}^{(\zeta)}(\xi). \tag{B12}$$

The matrix T is defined by $T^{(\zeta)}(\mathbf{k},\xi)_{\nu\mu} = \hat{F}_{\nu,-\mu}^{(\zeta)}(\xi)e^{i\,\mathbf{k}\mathbf{e}_\nu}$.

3. Expression of the characteristic function

Introducing (B9) into (B6) directly gives

$$\lim_{\rho_0\to0}\frac{\hat{\psi}(\mathbf{k},\xi)}{\rho_0} = -\sum_{\nu}\left\{\frac{1}{1-\xi} - \left[\frac{1}{1-\xi} + \hat{\tilde{q}}_{-\nu}^{(\zeta)}(\mathbf{k},\xi)\right]e^{i\,\mathbf{k}\mathbf{e}_\nu}\right\}h_\zeta(\xi), \tag{B13}$$

$$h_\zeta(\xi) = \sum_{Z\notin\{X_i^0\}}\hat{F}_{\zeta,Z}(\xi) = \sum_{Z=X_\zeta^0+1}^{X_{\zeta+1}^0-1}\hat{F}_{\zeta,Z}(\xi) \tag{B14}$$

with $\hat{\tilde{q}}_\nu^{(\zeta)}$ given by (B12), and $\zeta = \zeta(\nu) = \nu$ if $\nu > 0$, $\zeta = -\nu - 1$ if $\nu < 0$.

4. Expression of the quantities of interest ($\hat{F}_{\nu,\eta}^{(\zeta)}$ and h_μ)

We first state two results (see Ref. [27]) that we use in the following:

(1) The Laplace transform of the first passage density at the origin at time t of a symmetric one-dimensional Polya walk starting from site l is

$$\hat{f}_l(\xi) = \alpha^{|l|} \quad \text{with} \quad \alpha = \frac{1-\sqrt{1-\xi^2}}{\xi}. \tag{B15}$$

(2) The Laplace transform of the probability of first passage at site s_1 starting from site s_0 and considering site s_2 as an absorbing site (i.e., the particle is trapped) is given by

$$\hat{F}^{\dagger}(s_1|s_0,\xi) = \frac{\hat{f}_{s_1-s_0}(\xi) - \hat{f}_{s_1-s_2}(\xi)\hat{f}_{s_2-s_0}(\xi)}{1-\hat{f}_{s_1-s_2}(\xi)^2}. \tag{B16}$$

Now we compute the quantities of interest. From (B15), we immediately obtain:

$$\hat{F}_{-1,-1} = \hat{F}_{+N,+N} = \alpha. \tag{B17}$$

From (B15) and (B16), and recalling that the distance between TP μ and TP $\mu+1$ is $L_\mu^{(\zeta)}$, we obtain

$$\hat{F}^{(\zeta)}_{\mu,\mu} = \hat{F}^{(\zeta)}_{-\mu+1,-\mu-1} = \frac{\alpha - \alpha^{2L_\mu^{(\zeta)}-1}}{1-\alpha^{2L_\mu^{(\zeta)}}}, \tag{B18}$$

$$\hat{F}^{(\zeta)}_{\mu,-\mu+1} = \hat{F}^{(\zeta)}_{-\mu+1,\mu} = \frac{\alpha^{L_\mu^{(\zeta)}-1} - \alpha^{L_\mu^{(\zeta)}+1}}{1-\alpha^{2L_\mu^{(\zeta)}}}. \tag{B19}$$

And the sums are

$$h_0 = h_N = \sum_{Z=1}^{\infty} \alpha^{|Z|} = \frac{\alpha}{1-\alpha}, \tag{B20}$$

$$h_\mu = \sum_{Z=1}^{L_\mu-1} \frac{\alpha - \alpha^{2L_\mu - Z}}{1-\alpha^{2L_\mu}} = \frac{\alpha(1-\alpha^{L_\mu-1})(1-\alpha^{L_\mu})}{(1-\alpha)(1-\alpha^{2L_\mu})}. \tag{B21}$$

Equation (B13) gives the Laplace transform of the characteristic function $\hat{\psi}$ in terms of $\hat{\tilde{q}}_\nu^{(\zeta)}$ and h_μ. h_μ is given by Eqs. (B20) and (B21). $\hat{\tilde{q}}_\nu^{(\zeta)}$ is expressed in terms of $\hat{F}^{(\zeta)}_{\mu,\nu}$ [Eq. (B12)], which are themselves given by Eqs. (B17)–(B19). Everything is now ready for the evaluation of the characteristic function.

APPENDIX C: RESULTS IN THE HIGH-DENSITY LIMIT

1. Scaling of the characteristic function

We are now able to prove the main result for the characteristic function at high density [Eq. (15)]. Using a numerical software (Mathematica) we inject Eq. (B12) and Eqs. (B17)–(B21) into Eq. (B13) to obtain the following expression for the discrete Laplace tranform of the second characteristic function:

$$\lim_{\rho_0\to 0} \frac{\hat{\psi}(\mathbf{k},\xi)}{\rho_0} = \frac{1}{(1-\alpha^2)(1-\xi)} \sum_{n=0}^{N-1}\sum_{i=1}^{N-n} \alpha^{\mathcal{L}_i^n} \big\{ 2\alpha(1-\alpha^{L_{i-1}})(1-\alpha^{L_{i+n}})\cos(k_i+\cdots+k_{i+n}) + (1-\alpha)Q_n(k_i,\ldots,k_{i+n}) + C_{i,n} \big\} \tag{C1}$$

with $\alpha = \xi^{-1}(1-\sqrt{1-\xi^2})$. $C_{i,n}$ are constants enforcing that the brackets are zero when $\mathbf{k}=\mathbf{0}$, so that $\hat{\psi}(\mathbf{k}=\mathbf{0})=0$. We also defined

$$\mathcal{L}_i^n = L_i + \cdots + L_{i+n-1}, \tag{C2}$$

$$Q_2(k_1,k_2) = \alpha^{L_1}(e^{ik_1}+e^{-ik_2}), \tag{C3}$$

$$Q_3(k_1,k_2,k_3) = \alpha^{L_1}(e^{ik_1}+e^{-ik_2}) + \alpha^{L_2}(e^{ik_2}+e^{-ik_3}) + \alpha^{L_1+L_2}(e^{i(k_1+k_2)}+e^{-i(k_2+k_3)}+2\cos k_2). \tag{C4}$$

Similar expressions exist for $Q_n, n>3$. We will see that they do not contribute to the asymptotic scaling.

We define the total length $L = L_1+\cdots+L_{N-1}$ and the rescaled variables $\lambda_i^{(n)} = \mathcal{L}_i^n/L$.

We define $p = 1-\xi$ (continuous Laplace variable) and $\tilde{p} = pL^2$ (rescaled continuous Laplace variable). We take the limit $p\to 0$ keeping $\tilde{p}$ constant. This is a limit of large time.

The asymptotic behavior of α is given by

$$\alpha = \frac{1-\sqrt{1-\xi^2}}{\xi} = 1-\sqrt{2p}+\mathcal{O}_{p\to 0}(p), \tag{C5}$$

so that (r is an arbitrary number)

$$\alpha^{rL} \underset{p\to 0}{\sim} e^{-r\sqrt{2\tilde{p}}}. \tag{C6}$$

Equation (C1) becomes

$$\lim_{\rho_0\to 0}\frac{\hat{\psi}(\mathbf{k},p=L^2\tilde{p})}{\rho_0}\underset{p\to 0}{\sim}\frac{L^3}{\sqrt{2}\tilde{p}^{3/2}}\sum_{n=0}^{N-1}\sum_{i=1}^{N-n}(e^{-\sqrt{2\tilde{p}}\,\lambda_i^{(n)}}-e^{-\sqrt{2\tilde{p}}\,\lambda_{i-1}^{(n+1)}}-e^{-\sqrt{2\tilde{p}}\,\lambda_i^{(n+1)}}+e^{-\sqrt{2\tilde{p}}\,\lambda_{i-1}^{(n+2)}})$$
$$\times\,[\cos(k_i+\cdots+k_{i+n})-1]. \tag{C7}$$

The following continuous inverse Laplace tranform is known:

$$\hat{h}(p)=\frac{e^{-r\sqrt{2p}}}{p^{3/2}}\Leftrightarrow h(t)=2\sqrt{\frac{t}{\pi}}g\left(\frac{r}{\sqrt{2t}}\right), \tag{C8}$$
$$g(u)=e^{-u^2}-\sqrt{\pi}\,u\,\operatorname{erfc}(u). \tag{C9}$$

Expression (C7) can then be Laplace-inverted, the limit $p\to 0$ becomes $t\to\infty$, and we find

$$\lim_{\rho_0\to 0}\frac{\psi(\mathbf{k},t)}{\rho_0}\underset{t\to\infty}{\sim}\sqrt{\frac{2t}{\pi}}\sum_{n=0}^{N-1}\sum_{i=1}^{N-n}\left[g\left(\frac{\lambda_i^{(n)}}{\sqrt{2\tau}}\right)-g\left(\frac{\lambda_{i-1}^{(n+1)}}{\sqrt{2\tau}}\right)-g\left(\frac{\lambda_i^{(n+1)}}{\sqrt{2\tau}}\right)+g\left(\frac{\lambda_{i-1}^{(n+2)}}{\sqrt{2\tau}}\right)\right]$$
$$\times\,[\cos(k_i+\cdots+k_{i+n})-1]. \tag{C10}$$

We defined the rescaled time $\tau=t/L^2$. This result is Eq. (15).

2. Large deviation function for a single TP

For completeness, we write explicitly the large deviation function for a single TP with our high-density approach and show that it is consistent with the results (given at arbitrary density) of Ref. [15]. Note that this large deviation function is the one involved in the displacement of the center of mass at very large time [Eq. (18)].

For a single tracer at high density our approach (which coincides with Ref. [14]) gives

$$\psi(k,t)=\rho_0\sqrt{\frac{2t}{\pi}}(\cos k-1). \tag{C11}$$

The Gärtner-Ellis theorem [28] writes

$$P\left(Y=\rho_0\sqrt{\frac{2t}{\pi}}y\right)\asymp e^{-\rho_0\sqrt{\frac{2t}{\pi}}I_0(y)} \tag{C12}$$
$$I_0(y)=\sup_{q\in\mathbb{R}}[qy-(\cosh q-1)]. \tag{C13}$$

Solving for the extremum gives

$$e^{\pm q}=\pm y+\sqrt{1+y^2} \tag{C14}$$

and finally

$$I_0(y)=1-\sqrt{1+y^2}+y\ln[y+\sqrt{1+y^2}]. \tag{C15}$$

Limit of the general large deviation function

We check that the previous result is consistent with the general expression obtained in Ref. [15]. Adopting our notations, the results of Ref. [15] read

$$P(Y=\sqrt{t}y)\asymp e^{-\sqrt{t}I(y)}, \tag{C16}$$
$$I(y)=\mu(-y/\sqrt{2},\lambda^*) \tag{C17}$$

with

$$\frac{\partial\mu}{\partial\lambda}(\xi,\lambda^*)=0, \tag{C18}$$
$$\mu(\xi,\lambda)=\sum_{n=1}^{\infty}\frac{(-\omega)^n}{\sqrt{\pi}n!}g(\sqrt{n}\xi)+\xi\ln\left[\frac{1+\rho(e^{\lambda}-1)}{1-\rho(e^{-\lambda}-1)}\right], \tag{C19}$$
$$\omega=2\rho(1-\rho)(\cosh\lambda-1). \tag{C20}$$

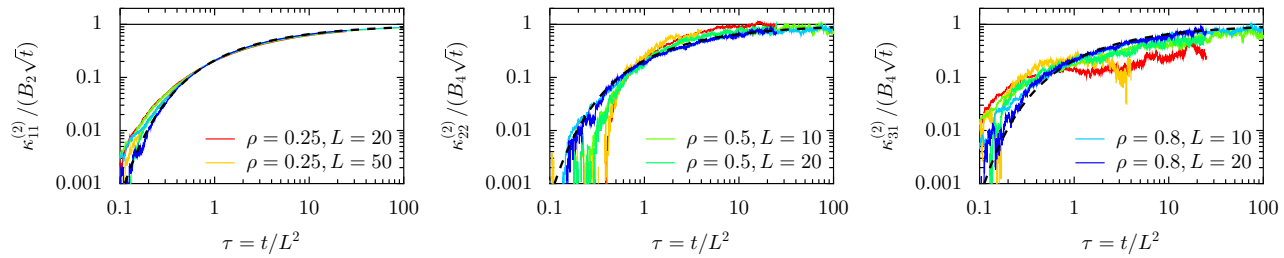

FIG. 7. Evolution of the cumulants associated to two TPs at different densities and different distances. The cumulants are rescaled by the single-tag cumulants, following (C25). The dashed line corresponds to $g((2\tau)^{-1/2})$.

We now consider the limit of high density $\rho = 1 - \rho_0$ with $\rho_0 \ll 1$. In this case the deviations scale with ρ_0: we are led to define the rescaled variable $\tilde{\xi} = \xi/\rho_0$. The limit $\rho \to 0$ of μ is then given by

$$\lim_{\rho_0 \to 0} \frac{\mu(\rho_0 \tilde{\xi}, \lambda)}{\rho_0} = -\frac{2}{\sqrt{\pi}}(\cosh \lambda - 1) + 2\tilde{\xi}\lambda. \tag{C21}$$

The optimization over λ is performed as before and gives

$$e^{\pm\lambda^*} = \pm\sqrt{\pi}\tilde{\xi} + \sqrt{1 + \pi\tilde{\xi}^2}, \tag{C22}$$

$$\lim_{\rho_0 \to 0} \frac{\mu(\rho_0 \tilde{\xi}, \lambda^*)}{\rho_0} = -\frac{2}{\sqrt{\pi}}\left[\sqrt{1 + \pi\tilde{\xi}^2} - 1\right] + 2\tilde{\xi} \ln\left(\sqrt{\pi}\tilde{\xi} + \sqrt{1 + \pi\tilde{\xi}^2}\right). \tag{C23}$$

Eventually one obtains the high-density limit of the large deviation function I:

$$\lim_{\rho_0 \to 0} \frac{I\left(\rho_0 \sqrt{\frac{2}{\pi}} u\right)}{\rho_0 \sqrt{\frac{2}{\pi}}} = \sqrt{\frac{\pi}{2}} \lim_{\rho_0 \to 0} \frac{\mu(-\rho_0 \pi^{-1/2} u, \lambda^*)}{\rho_0} = I_0(u). \tag{C24}$$

I_0 was defined in Eq. (C15). We indeed recovered the result of Eq. (C12).

3. Numerical verification of the expression of $\kappa_{11}^{(2)}$ at arbitrary density

For the Edwards-Wilkinson dynamics, the correlation $\kappa_{11}^{(2)}$ (at any density ρ) is known to be given by [31]

$$\kappa_{11}^{(2)} = \kappa_2^{(1)} g\left(\frac{1}{\sqrt{2\tau}}\right) = \frac{1 - \rho}{\rho}\sqrt{\frac{2t}{\pi}} g\left(\frac{1}{\sqrt{2\tau}}\right). \tag{C25}$$

We check here that this behavior is actually in good agreement with numerical simulations of the SEP in continuous time (see Fig. 7, left).

4. Argument for the breaking of our scaling form at arbitrary density

The Edwards-Wilkinson dynamics is a Gaussian model and thus cannot give the time evolution of arbitrary cumulants. For arbitrary cumulants, we showed that

$$\lim_{t \to \infty} \frac{\kappa_{p_1, \ldots, p_N}^{(N)}}{\sqrt{t}} = \lim_{t \to \infty} \frac{\kappa_{p_1 + \cdots + p_N}^{(1)}}{\sqrt{t}} = B_{p_1 + \cdots + p_N}, \tag{C26}$$

where the constants B_k characteristic of a single tracer have been determined in Ref. [15].

Here we demonstrate that our scaling form [function $g((2\tau)^{-1/2})$] cannot be valid for arbitrary cumulants at arbitrary density. Indeed, the results of Ref [15] and our results for the probability law of the distance (that are consistent with numerical simulations) would disagree if it were the case.

In analogy with (C25), we would like to be able to make the following bold conjecture:

$$\kappa_{p,2n-p}^{(2)} = B_{2n}\sqrt{t}\, g((2\tau)^{-1/2}).$$

Unfortunately we show that this is incompatible with the law of the distance (A6).

Let us focus on the fourth cumulant of the distance (we denote $\langle \cdot \rangle_c$ the cumulants):

$$\langle (X_2 - X_1)^4 \rangle_c = \langle X_1^4 \rangle_c + \langle X_2^4 \rangle_c - 4\langle X_1^3 X_2 \rangle_c - 4\langle X_1 X_2^3 \rangle_c + 6\langle X_1^2 X_2^2 \rangle_c. \tag{C27}$$

We *assume*, according to our hypothesis, that

$$\langle X_1^4 \rangle_c = \langle X_2^4 \rangle_c = B_4 \sqrt{t} + o(1), \tag{C28}$$

$$\langle X_1^3 X_2 \rangle_c = \langle X_1 X_2^3 \rangle_c = \langle X_1^2 X_2^2 \rangle_c = B_4 \sqrt{t}\, g\left(\frac{1}{\sqrt{2\tau}}\right) = B_4 \sqrt{t} - B_4 \sqrt{\frac{\pi}{2}} L + o(1). \tag{C29}$$

This leads us to

$$\langle (X_2 - X_1)^4 \rangle_c = \sqrt{2\pi}\, B_4 L + o(1). \tag{C30}$$

Reference [15] gives the coefficient B_4:

$$B_4 = \sqrt{\frac{2}{\pi}} \frac{1-\rho}{\rho^3} \left\{ 1 - [4 - (8 - 3\sqrt{2})\rho](1-\rho) + \frac{12}{\pi}(1-\rho)^2 \right\}, \tag{C31}$$

while from (A6) or from the generating function (A12),

$$\langle (X_2 - X_1)^4 \rangle_c \underset{L\to\infty}{\sim} 2L \frac{1-\rho}{\rho^3}(12 - 24\rho + 13\rho^2). \tag{C32}$$

At an arbitrary density, this is inconsistent with (C30), thus our conjecture must be wrong. Note that (C30) does hold as expected when $\rho \to 1$.

In Fig. 7 center (resp. right), we tried the following guess: $\kappa_{22}^2 = B_4 \sqrt{t}\, g[(2\tau)^{-1/2}]$ (resp. $\kappa_{31}^2 = B_4 \sqrt{t}\, g[(2\tau)^{-1/2}]$). We see that it is valid only at high density, as expected.

APPENDIX D: DESCRIPTION OF NUMERICAL SIMULATIONS

We now describe the two kinds of numerical simulations that we performed: the continuous-time simulations to obtain the cumulants, and the vacancy-based discrete simulations in discrete time to obtain the joint probability law.

1. Continuous-time simulations on a lattice (for the cumulants)

N_{parts} particles are put uniformly at random on the line of size N_{size}, except the N-tagged particles, which are put deterministically on their initial positions. We used $N_{\text{size}} = 5000$

Each particle has an exponential clock of time constant $\tau = 1$. Thus, the whole system has an exponential clock of time constant $\tau_{\text{all}} = \tau / N_{\text{parts}}$. When it ticks, a particle is chosen at random and tries to move either to the left or to the right with probability $1/2$. If the arrival site is already occupied, the particle stays where it was.

The cumulants of the N TPs are averaged over 100 000 to 500 000 simulations to obtain their time dependence (Fig. 3).

2. Vacancy-based simulations (for the probability distribution)

The previous approach does not enable one to get sufficient statistics to investigate the probability law.

In the case of ponctual Brownian particles, Ref. [21] was able to use the propagator of the displacement to directly obtain the state of the system at a given time and investigate the probability distribution.

Here we used a numerical scheme close to our theoretical approach: at high density and in discrete time, we simulate the behavior of the vacancies considered as an independent random walker. The displacement Δx of a vacancy at (discrete) time t is given by a binomial law:

$$\Delta x = 2n_{\text{right}} - t, \tag{D1}$$

$$P(n_{\text{right}}, t) = \frac{1}{2^t} \binom{t}{n_{\text{right}}}. \tag{D2}$$

One is able to recover the final positions of the TPs from the final positions of the vacancies.

For two TPs at distance L, we put a vacancy at each site between the TPs with probability ρ_0 (density of vacancies). We consider a number of sites N_{sites} ($N_{\text{sites}} = 100\,000$) on the left of the first TP and on the right of the second TP, and we put a deterministic number of vacancies $N_{\text{vac}} = \rho_0 N_{\text{sites}}$ at random positions on these sites.

We make 10^8 repetitions of the simulation before outputting the probability law (Fig. 2).

[1] T. E. Harris, J. Appl. Probab. **2**, 323 (1965).

[2] V. Gupta, S. S. Nivarthi, A. V. McCormick, and H. T. Davis, Chem. Phys. Lett. **247**, 596 (1995).

[3] K. Hahn, J. Kärger, and V. Kukla, Phys. Rev. Lett. **76**, 2762 (1996).

[4] Q.-H. Wei, C. Bechinger, and P. Leiderer, Science **287**, 625 (2000).

[5] T. Meersmann, J. W. Logan, R. Simonutti, S. Caldarelli, A. Comotti, P. Sozzani, L. G. Kaiser, and A. Pines, J. Phys. Chem. A **104**, 11665 (2000).

[6] B. Lin, M. Meron, B. Cui, S. A. Rice, and H. Diamant, Phys. Rev. Lett. **94**, 216001 (2005).
[7] D. G. Levitt, Phys. Rev. A **8**, 3050 (1973).
[8] P. A. Fedders, Phys. Rev. B **17**, 40 (1978).
[9] S. Alexander and P. Pincus, Phys. Rev. B **18**, 2011 (1978).
[10] R. Arratia, Ann. Probab. **11**, 362 (1983).
[11] L. Lizana, T. Ambjörnsson, A. Taloni, E. Barkai, and M. A. Lomholt, Phys. Rev. E **81**, 051118 (2010).
[12] A. Taloni and M. A. Lomholt, Phys. Rev. E **78**, 051116 (2008).
[13] G. Gradenigo, A. Puglisi, A. Sarracino, A. Vulpiani, and D. Villamaina, Phys. Scr. **86**, 058516 (2012).
[14] P. Illien, O. Bénichou, C. Mejía-Monasterio, G. Oshanin, and R. Voituriez, Phys. Rev. Lett. **111**, 038102 (2013).
[15] T. Imamura, K. Mallick, and T. Sasamoto, Phys. Rev. Lett. **118**, 160601 (2017).
[16] S. F. Burlatsky, G. Oshanin, M. Moreau, and W. P. Reinhardt, Phys. Rev. E **54**, 3165 (1996).
[17] C. Landim, S. Olla, and S. B. Volchan, Commun. Math. Phys. **192**, 287 (1998).
[18] S. Majumdar and M. Barma, Physica A (Amsterdam) **177**, 366 (1991).
[19] R. Rajesh and S. N. Majumdar, Phys. Rev. E **64**, 036103 (2001).
[20] J. Cividini, A. Kundu, S. N. Majumdar, and D. Mukamel, J. Stat. Mech. (2016) 053212.
[21] S. Sabhapandit and A. Dhar, J. Stat. Mech. (2015) P07024.
[22] M. J. A. M. Brummelhuis and H. J. Hilhorst, Physica A (Amsterdam) **156**, 575 (1989).
[23] O. Bénichou and G. Oshanin, Phys. Rev. E **66**, 031101 (2002).
[24] O. Bénichou, A. Bodrova, D. Chakraborty, P. Illien, A. Law, C. Mejía-Monasterio, G. Oshanin, and R. Voituriez, Phys. Rev. Lett. **111**, 260601 (2013).
[25] P. Illien, O. Bénichou, G. Oshanin, and R. Voituriez, Phys. Rev. Lett. **113**, 030603 (2014).
[26] O. Bénichou, P. Illien, G. Oshanin, A. Sarracino, and R. Voituriez, Phys. Rev. Lett. **115**, 220601 (2015).
[27] B. D. Hughes, *Random Walks and Random Environments* (Oxford University Press, Oxford, 1995), Vol. 1.
[28] H. Touchette, Phys. Rep. **478**, 1 (2009).
[29] H. Spohn, J. Phys. A **16**, 4275 (1983).
[30] S. Gupta, S. N. Majumdar, C. Godrèche, and M. Barma, Phys. Rev. E **76**, 021112 (2007).
[31] P. L. Krapivsky, S. Redner, and E. Ben-Naim, *A Kinetic View of Statistical Physics* (Cambridge University Press, Cambridge, 2009).